Fine Structure of the 3^2P and 4^2P States of Lithium†

R. C. Isler,* S. Marcus,‡ and R. Novick§
Columbia Radiation Laboratory, Department of Physics, Columbia University, New York, New York 10027
(Received 16 June 1969)

The fine-structure intervals of the 3^2P state of Li^6 and Li^7 and the 4^2P state of Li^7 have been measured by observing the level crossing signals from the $P_{3/2}{}^{-3/2}$ and $P_{1/2}{}^{1/2}$ levels. Results for the magnetic fields at which the center of the crossing signals occur are the following, in terms of the proton NMR frequency in kHz for a mineral oil sample: $3^2P(Li^7)$, 3897.163(22); $3^2P(Li^6)$, 3896.89(20); $4^2P(Li^7)$, 1621.71(15). By using a theory of the Zeeman effect that includes estimates of the normal and specific mass effects and relativistic effects, we find the following values for the zero-field fine-structure intervals: $\Delta W(Li^7 - 3P) = 2882.903(18)$ MHz; $\Delta W(Li^7 - 4P) = 1199.65(11)$ MHz. The uncertainties are three times the standard error for the measurement.

I. INTRODUCTION

The fine structures of excited P states of the lithium atom have been the object of both theoretical and experimental investigations within the last few years. Comparisons between theoretical calculations and experimental measurements on the structures of simple atoms provide valuable tests of various theoretical approaches which may prove useful for all atoms. In particular, methods of computing spin-orbit interactions for electrons can be tested by comparison of calculated and measured values of fine-structure intervals. Lithium provides a case of particular interest for evaluating these interactions; spin-orbit interactions between electrons are responsible for the fine-structure intervals being smaller in lithium than the corresponding intervals in hydrogen. This result is unexpected if one considers the incomplete Coulomb shielding of the nucleus by the core electrons as the only correction to hydrogenic spin-orbit theory. The incomplete shielding tends to increase the fine-structure separation because the effective charge is greater than unity. Bell,[1] and Bell and Stewart,[2] have explored the usefulness of two types of approximate wave functions for calculating the separations of ^2P terms in the lithium isoelectronic sequence up to $Z = 9$. They have used variational wave functions of the open-shell type and Hartree-Fock wave functions which satisfy the cusp condition, and they indicate that the latter produce satisfactory agreement for the heavier members of the sequence. For the lightest member, lithium, in which electron-electron interactions are the most important, the agreement is very poor.

Brog, Wieder, and Eck[3] have recently exploited the technique of level crossing spectroscopy to measure the 2^2P interval in Li^6 and Li^7. Their results are accurate to about 2 parts in 10^5. In a similar type of investigation, Budick *et al.*[4] first observed level crossing signals in the 3^2P state of Li^7, although they did not try to obtain high precision for the fine-structure interval. The present work has refined the measurement of the 3^2P state, and extended the scope of work in lithium to the 4^2P state. It is hoped that the availability of these accurate measurements for lithium will encourage continued theoretical work directed toward improved calculations for two-electron operators in atomic structures.

II. THEORY

Level crossing spectroscopy has proved to be a very useful technique for the study of lifetimes and structures of excited states in atoms. The principles are well known, but a brief description of details related to the present experiments will be given.

An energy-level diagram of the lower-lying states of lithium is shown in Fig. 1, in which the wavelengths of the first three $n^2P \rightarrow 2^2S$ resonance transitions are indicated. Our present experiments have been performed on 3^2P and 4^2P states in which certain sublevels of the $J = \frac{3}{2}$ and $J = \frac{1}{2}$ states are made to cross in a magnetic field. The $P_{3/2}{}^{-3/2}$ level can be made degenerate with either the $P_{1/2}{}^{1/2}$ level or $P_{1/2}{}^{-1/2}$ level depending upon the value of the magnetic field. The selection rule, $\Delta m_J = 0, \pm 1$, for electric dipole radiation implies that magnetic sublevels differing in m_J by 0, 1, or 2 can be excited coherently by absorbing a photon of a given energy and polarization from a source which produces the resonance lines. In the reradiated light, interference effects may occur which depend on the ratio of the energy separation of the two excited states to their natural linewidth. If the levels are much farther apart in energy than a few natural linewidths, the interference effects are negligible compared to the isotropic background, but if these levels are almost

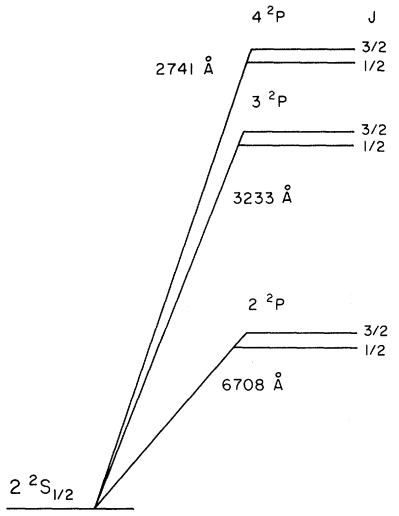

FIG. 1. Energy-level diagram for the first three resonance transitions in lithium.

degenerate, the interference effects show up quite strongly. The absorption and reemission process is described by the Breit formula,[5]

$$R \propto \sum_{mm',\mu\mu'} \frac{f_{\mu m} f_{m\mu'} g_{\mu' m'} g_{m'\mu}}{\Gamma^2 + [(E_\mu - E_{\mu'})/\hbar]^2} \times [\Gamma - i(E_\mu - E_{\mu'})/\hbar] \ , \qquad (1)$$

where $f_{\mu m} = (\mu | \vec{f} \cdot \vec{r} | m)$ and $g_{\mu m} = (\mu | \vec{g} \cdot \vec{r} | m)$, the matrix elements for electric dipole transitions. The polarization vectors of the exciting and reradiated light are denoted, respectively, by $\vec{f}$ and $\vec{g}$; m and m' denote the ground-state sublevels; and μ and μ' denote the excited-state sublevels. The term $(E_\mu - E_{\mu'})$ represents the separation of the excited levels, and Γ is the average of their natural widths. For fixed directions of the exciting and reradiated light beams, a change in intensity of the scattered light is observed as $(E_\mu - E_{\mu'})$ is varied by sweeping the magnetic field.

A detailed diagram of the $\delta m_J = 2$ crossing levels is shown in Fig. 2 for Li^7. The hyperfine structure is explicitly indicated for this isotope which has a nuclear spin of $\frac{3}{2}$. Only the $\delta m_J = 2$ level crossings have been measured in the present work because the individual hyperfine crossing signals are much better resolved than they are for the $\delta m_J = 1$ crossings. The $P_{3/2}{}^{-3/2}$ and $P_{1/2}{}^{1/2}$ levels can be coherently excited only from the $S_{1/2}{}^{-1/2}$ level of the ground state, and the observed radiation is that of the resonance line itself so that the computation from the Breit formula is rather simple. Strong interference effects occur when the two levels which cross have the same value of m_I. Four level crossing signals are, therefore, produced in Li^7 when the magnetic field is swept through a small range. In Li^6, which has nuclear spin of 1, only three crossings occur. Anticrossings also occur within the complex of crossings for states that have the same value of m_F.[6] The anticrossing between these two states arises from electric quadrupole interactions and second-order magnetic-dipole interactions. A detailed calculation using the Breit formula indicates that the effects of these anticrossings can be ignored in the present experiments; i.e., the centers of all the level crossing signals occur, within 1 ppm, at the same magnetic field at which they would occur if there were no anticrossings.

The analysis of the fields measured at the center of the level crossing signals in order to obtain the fine-structure interval is accomplished in two steps: (i) The fields at which the individual hyperfine crossings occur are corrected to obtain the magnetic field H_C (in terms of measured proton-resonance frequencies) at which the two fine-structure sublevels would cross if there were no hyperfine interaction present; (ii) H_C is related to the zero-field fine-structure interval by using a suitably accurate theory for the Zeeman effect. The first step in this procedure is accomplished in a straightforward manner; it will be seen that only second-order hyperfine corrections are necessary so that a knowledge of the interaction constants to a few percent is adequate. The relation

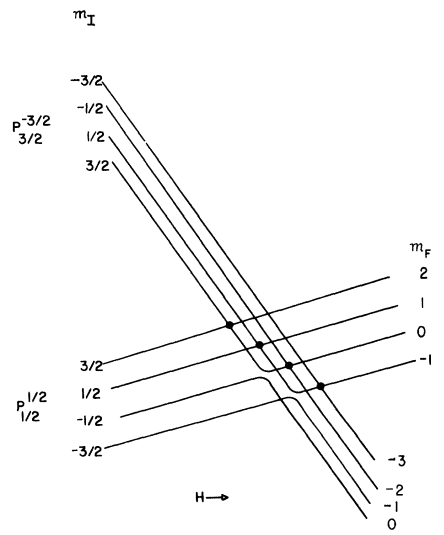

FIG. 2. Energy-level configuration for $\delta m = 2$ crossings between $^2P_{1/2}{}^{1/2}$ and $^2P_{3/2}{}^{-3/2}$ states. The four hyperfine level-crossing signals occur at positions indicated by solid circles. Two anticrossings also occur for states with the same value of m_F.

of H_c to the fine-structure interval requires estimates of various corrections to the g values, such as normal and specific mass effects and relativistic corrections.

The magnetic field H_c is related to the measured fields at which the crossings occur by calculating all matrix elements within the doublet for a Hamiltonian which contains operators for the fine structure, the Zeeman effect, and important hyperfine interactions. The Hamiltonian is split into two parts,

$$\begin{aligned} &\mathcal{H} = \mathcal{H}(1) + \mathcal{H}(2) \ , \\ &\mathcal{H}(1) = F + g_L \mu_0 \vec{L} \cdot \vec{H}_c + g_S \mu \vec{S} \cdot \vec{H}_c \ , \end{aligned} \tag{2}$$

where F is the fine-structure operator, and H_c is the magnetic field at which the level crossing would take place in the absence of any hyperfine structure, and

$$\mathcal{H}(2) = \mathcal{H}_d + \mathcal{H}_s + \mathcal{H}_z + \mathcal{H}_q - g_I \mu_N \vec{I} \cdot \vec{H} \ , \tag{3}$$

where $\mathcal{H}_d$ is the dipole-dipole hyperfine interaction of the valence electron and the nucleus, $\mathcal{H}_S$ is the core-polarization term, $\mathcal{H}_z$ is a Zeeman term $\mu_0 \Delta H_i (g_L L_z + g_S S_z)$, that accounts for the fact that the ith hyperfine crossing takes place at a magnetic field that differs from H_c by ΔH_i, $\mathcal{H}_q$ is the electric quadrupole interaction, and the final term accounts for the nuclear Zeeman effect.

The magnetic field interaction strongly couples states of the doublet which have the same value of m_J. The calculational procedure, therefore, has been to diagonalize $\mathcal{H}(1)$ and to use the resultant eigenstates to compute first- and second-order perturbations due to $\mathcal{H}(2)$. For the level crossings observed, diagonalization of $\mathcal{H}(1)$ leads to the relationship

$$\mu_0 H_c = [(g_S + 2g_L)/3g_L(g_S + g_L)] \Delta W \ , \tag{4}$$

where ΔW is the fine-structure interval. A more explicit outline of the calculation is found in the Appendix.

The level crossing signals are centered at the point where the difference in energy is zero between the two levels with the same values of m_I. The important terms in these differences which relate ΔH_i and the hyperfine interactions are shown in Table I for each of the four crossings. The constants $a_{d3/2}$ and $a_{d1/2}$ are the hyperfine dipole-dipole coupling constants for the $J = \frac{3}{2}$ and $J = \frac{1}{2}$ states, a_c is the coupling constant for the core-polarization term, and b is the quadrupole-coupling constant. The second-order terms have been computed with the assumption that the radial wave functions of all states of the doublet are identical so that the relative values of the dipole-dipole coupling constants depend only on the angular-momentum quantum numbers for the two states, with the result that $a_{d1/2} = 5a_{d3/2}$. The assumption that the coupling constants of different states of a multiplet are related only by angular-momentum quantum numbers is known to be incorrect for F^{19} and O^{17} in which deviations as great as 13% have been found from calculated ratios.[7] A difference of 13% in the ratio of $a_{d1/2}$ to $a_{d3/2}$ in the present experiments would lead to a shift of 1.5 ppm in our final results for H_c.

If the relationships for the two outer and two inner pairs of crossings from Table I are added, the first-order magnetic-dipole terms are elim-

TABLE I. Theoretical relationships between hyperfine constants and magnetic fields at which level crossings occur. Here $E_H = \frac{1}{11}[20a_{d3/2} + 5a_{d1/2} + 6a_c]$.

M_I	
$\frac{3}{2}$	$-\frac{3}{2}E_H + \frac{3}{22}b - 2.182\mu_0\Delta H_1 + (3/2\Delta W)[0.38a_{d3/2}^2 + 6.24a_c^2$
	$+ 0.081\mu_0^2\Delta H_1^2 - 13.55a_{d3/2}a_c - 0.046a_{d3/2}\mu_0\Delta H_1 + 0.73a_c\mu_0\Delta H_1] = 0$
$\frac{1}{2}$	$-\frac{1}{2}E_H - \frac{3}{22}b - 2.182\mu_0\Delta H_2 + (3/2\Delta W)[-38.35a_{d3/2}^2 + 5.39a_c^2$
	$+ 0.081\mu_0^2\Delta H_2^2 - 2.17a_{d3/2}a_c - 0.015a_{d3/2}\mu_0\Delta H_2 + 0.26a_c\mu_0\Delta H_2] = 0$
$-\frac{1}{2}$	$+\frac{1}{2}E_H - \frac{3}{22}b - 2.182\mu_0\Delta H_3 + (3/2\Delta W)[-51.43a_{d3/2}^2 + 3.56a_c^2$
	$+ 0.081\mu_0^2\Delta H_3^2 + 7.50a_{d3/2}a_c + 0.015a_{d3/2}\mu_0\Delta H_3 - 0.26a_c\mu_0\Delta H_3] = 0$
$-\frac{3}{2}$	$+\frac{3}{2}E_H + \frac{3}{22}b - 2.182\mu_0\Delta H_4 + (3/2\Delta W)[-38.84a_{d3/2}^2 + 0.72a_c^2$
	$+ 0.081\mu_0^2\Delta H_4^2 + 15.44a_{d3/2}a_c + 0.046a_{d3/2}\mu_0\Delta H_4 - 0.73a_c\mu_0\Delta H_4] = 0$

inated, leaving two relationships for the ΔH_i's. H_c is then obtained by noting that $\frac{1}{2}(2H_c + \Delta H_1 + \Delta H_4)$ is the average of the measurements of the outer pair of crossings, and $\frac{1}{2}(2H_c + \Delta H_2 + \Delta H_3)$ is the average of the inner pair. Clearly, the measurements must be corrected only by the electric-quadrupole terms and the second-order magnetic-dipole terms in order to obtain H_c.

The values for $a_{d1/2}$, $a_{d3/2}$, a_c, and b are obtained by relating the measured level crossing intervals from both the high-field experiments and a separate low-field experiment to the theoretical calculations, then employing certain scaling assumptions that permit correlation with a double-resonance experiment in the 2^2P state of lithium.[8] The details of this analysis on the hyperfine structure are discussed in the following paper.[9] The following values from our analysis of the hyperfine structure have been used to obtain in MHz the second-order corrections: $a_{d3/2} = 2.11(3)$, $a_c = -3.08(3)$, $b = -0.018(22)$.

III. EXPERIMENTAL APPARATUS AND PROCEDURE

The most important features of the experimental arrangement are illustrated in Fig. 3. There are four principal components of the system: (i) a light source for optical excitation, (ii) a source for producing the lithium vapor which absorbs and reradiates the light, (iii) apparatus for producing and measuring the magnetic field, and (iv) equipment for detecting the reradiated light signal. Certain aspects of construction and procedures for making measurements are discussed in detail.

A flow lamp of the type described by Budick, Novick, and Lurio[10] has been used as the excitation source. A lithium beam is produced from a molybdenum oven which contains a spiral-wound crinkled molybdenum foil plug. This plug effectively provides a closely packed structure of narrow apertures through which a dense beam of vapor diffuses from the oven. A flow of argon is maintained through the quartz lamp jacket in a direction that prevents lithium from reaching the window. Hot lithium attacks quartz readily, causing small fissures or cracks, and it is necessary to shield the inside of the jacket near the oven with some material such as molybdenum foil. The lamp is excited by a 20–40-MHz rf oscillator. Considerable improvement in the intensity and stability of the light is obtained by passing the argon through a titanium-sponge getter before it enters the lamp. This getter has been operated at about 900 °C and is particularly good for absorbing molecular gases which otherwise decrease the intensity of the lamp.

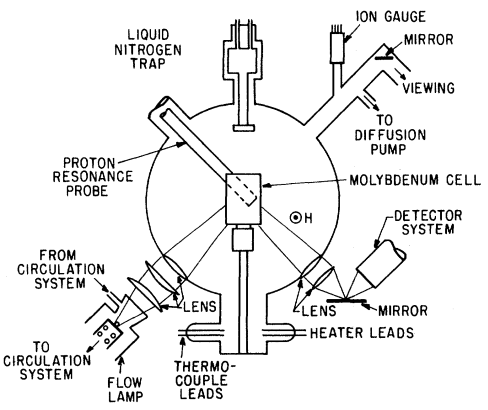

FIG. 3. Schematic diagram of apparatus. The resonance probe is retracted about 1 in. from the center of the cell while taking data.

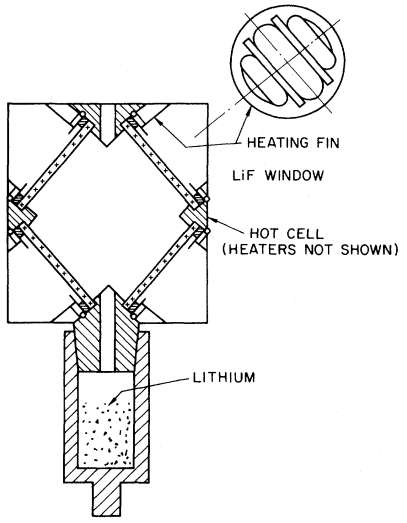

FIG. 4. Detailed view of scattering cell.

Because hot lithium degrades quartz and other materials so rapidly, no attempt has been made to contain the absorbing vapor in a closed cell. Instead, the scattering is done within a leaky molybdenum cell of the type shown in Fig. 4. Heaters are placed only in the upper part of the cell, which contains the entrance and exit windows for the light beam. The power for the heater filaments is supplied from a 100-kHz oscillator in order to minimize undesirable magnetic fields in the scattering region. The entire scattering cell is contained in an evacuated oxygen-free high-conductivity copper enclosure as shown in Fig. 3. Light from the lamp is focused onto the vapor, and the light scattered at 90° is focused onto a mirror from which it is reflected through a light pipe to a photomultiplier tube.

Lithium metal is contained in a cup in the lower part of the cell, which is machined so that a press fit provides good thermal contact with the upper

section. The hot lithium vapor diffuses out of the cup in a beam of approximately 3 mm diam and escapes through a 3-mm aperture in the top of the cell to deposit on the cold finger of a liquid-nitrogen trap. The beam is made visible by resonant light scattered from the 6707 Å line, and can be observed through the windows of the cell. It does not appear to be broadened to more than 6 mm in the scattering region. Lithium fluoride windows have been found to work best in the cell. Blackened copper slates are placed over the windows, and the assembly is held in place by snap rings. Although hot lithium vapor strongly attacks quartz, it does not degrade the transmission of lithium fluoride rapidly. The copper slats are kept at the temperature of the upper part of the cell through direct thermal contact and are vital for efficient operation; they provide an effective baffle to inhibit radiative cooling of the windows and thereby minimize the rate at which lithium vapor is deposited. The operating time when using this cell has been as much as 40 h before the windows become opaque from the deposition of lithium.

All magnetic field measurements are performed in terms of the proton NMR frequency by using a marginal oscillator, frequency counter, and a probe filled with mineral oil. The field is modulated by ± 1 G at 30 Hz. The 12-in. pole pieces of the magnet have been set to obtain the maximum homogeneity over a small volume in the center of the gap by adjusting them to obtain the minimum decay rate in the wiggles from the NMR probe. This technique has proved quite satisfactory, and the maximum gradient of the field at the center of the gap is 0.003 G/mm at a field strength of 1000 G. An uncertainty of ± 2 ppm has been added to the final result for the crossing field in order to account for the uncertainty arising from inhomogeneity of the magnetic field.

The NMR probe is set in a reentrant holder midway between the pole faces and placed as near as possible to the scattering cell. As a result, it must be cooled with a constant circulation of air so that the resonance pattern remains sharp and strong. The strength of the magnetic field is recorded at several positions on the level crossing signal itself during the course of taking data. Corrections must be made to the fields measured during an experiment in order to obtain the actual field at the center of the cell. These corrections are accomplished by removing one window of the cell so that the probe may be moved directly into the scattering region. The difference in readings between the two positions is 0.151(4) kHz. This correction has been measured several times after changing the magnetic field to high or low values, and then returning to the field strength at which the level crossings take place. No change in the correction was observed. These measurements indicate that the hysteresis of the magnet did not affect the magnetic field distribution near the scattering region.

The level crossing signal is detected with a narrow-band phase-sensitive amplifier. A precise measurement requires a very good signal-to-noise ratio, which has usually necessitated a modulation of approximately one linewidth and a 10-sec time constant in the amplifier. The most precise data have been obtained by sweeping slowly over the center of an individual crossing several times, then moving on to another crossing and repeating the procedure. Detailed discussions of the effects of modulation, sweep rates, and optical alignment may be found elsewhere.[11]

IV. RESULTS

Measurements have been made of the fine-structure intervals in the 3^2P states of Li^6 and Li^7, and in the 4^2P state of Li^7. Typical examples of the level crossing data are shown in Fig. 5. The individual signals approximate derivatives of Lorentzian curves. The four hyperfine lines are seen to be resolved well enough for the 3^2P state of Li^7 that accurate positions of their centers can be obtained by measuring the field at which the signal level is zero. For the 4^2P state, the relative value of the linewidth and hyperfine separation is such that individual components overlap significantly and restrict the accuracy of the fine-structure measurement to be less than that of the 3^2P state. The data for Li^6 exhibit even poorer resolution, and the accuracy of the fine-structure measurement was limited to 50 ppm.

Shifts in the centers of signals are caused by lags through the output-filter circuit of the phase-sensitive detector. These shifts can be completely negated by sweeping over the signal through an increasing magnetic field, then through a decreasing magnetic field. The average of measurements made in this manner gives the true center of the line, provided the optical alignment is perfect. If the angle between the incident and scattered light beams is not exactly 90°, the level crossing signal is not antisymmetric and a simple average of the data for the two directions of sweep does not provide the true center of the curve. During the present investigations several sets of data distorted by optical misalignment and large sweep rates for the 3^2P state of Li^7 were obtained in the process of setting up the experiment. Some of these sets of distorted data have been corrected by using a theory for highly modulated signals; the corrections bring H_C measured from the distorted data to within 3 or 4 ppm of the best results obtained from undistorted signals.

The following results, expressed in terms of the proton resonance frequency in kHz, have been obtained for the magnetic fields at which the crossings take place in the 3^2P state of Li^7:

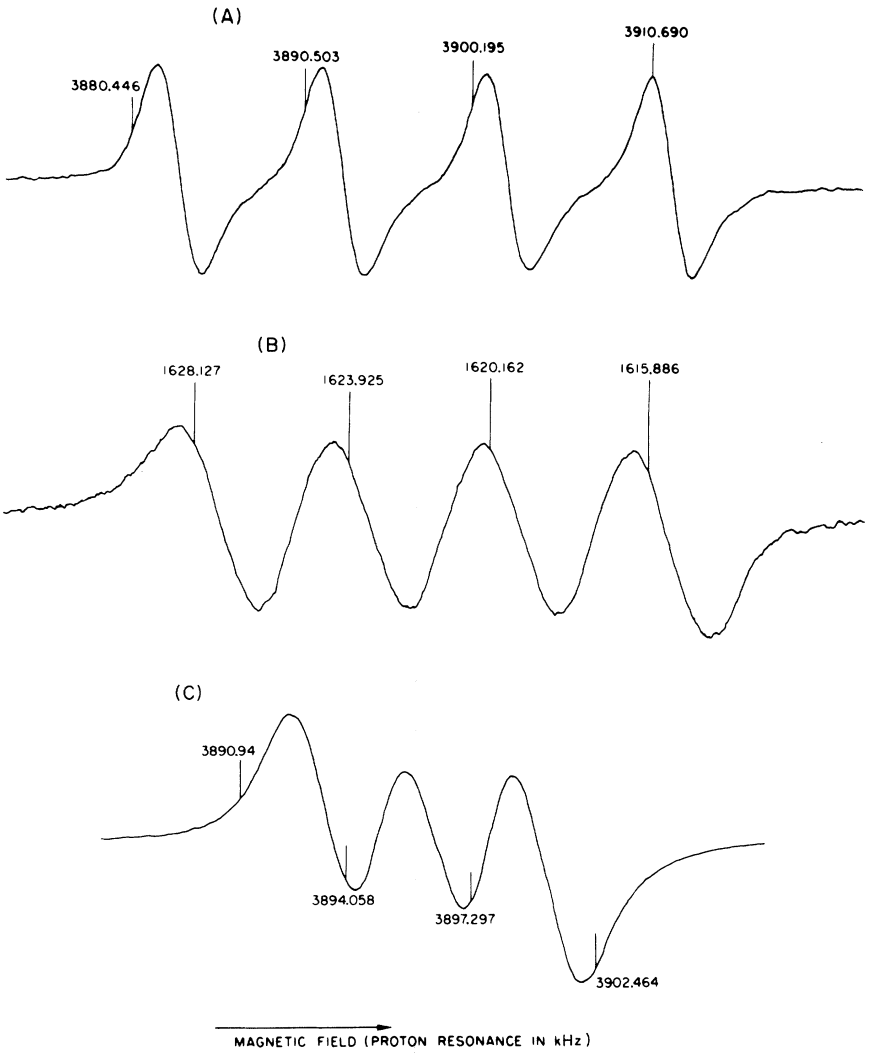

FIG. 5. Experimental results for $\delta m = 2$ level crossings; (a) 3^2P-Li^7; (b) 4^2P-Li^7; (c) 3^2P-Li^6. Field markers are in terms of the proton resonance frequency.

$$\begin{aligned} m_I &= \tfrac{3}{2}, \quad H_1 = 3882.726(13), \\ m_I &= \tfrac{1}{2}, \quad H_2 = 3892.244(15), \\ m_I &= \tfrac{1}{2}, \quad H_3 = 3901.835(14), \\ m_I &= \tfrac{3}{2}, \quad H_4 = 3911.527(15). \end{aligned} \tag{5}$$

The uncertainties represent three times the standard error from 10 sets of data. When the procedure outlined in Sec. II is applied to find H_C, the two outer crossings yield

$$\begin{aligned} H_C &= \tfrac{1}{2}(H_1 + H_4) + \text{second-order terms} \\ &= 3897.126(20) + 0.036(3)\ \text{kHz} \\ &= 3897.162(20)\ \text{kHz} \end{aligned} \tag{6}$$

and the two inner crossings give

$$\begin{aligned} H_C &= \tfrac{1}{2}(H_2 + H_3) + \text{second-order terms} \\ &= 3897.039(19) + 0.124(9)\ \text{kHz} \\ &= 3897.163(21)\ \text{kHz}. \end{aligned} \tag{7}$$

It is noteworthy that these results agree to within 1 Hz, even though the corrections differ by about 90 Hz. This agreement produces added confidence in the procedure. The average of these two values plus the inclusion of a 12-Hz uncertainty in the magnetic field to account for systematic errors in probe position and field inhomogeneity yield a final result:

$$H_C = 3897.163(22)\ \text{kHz}. \tag{8}$$

The stated error of about 6 ppm is considerably smaller than the 50 ppm obtained by Budick *et al.*, who reported a measurement of $H_C = 3897.2(2)$

kHz.

In order to determine the fine-structure splitting precisely from H_C, it is necessary to include the electrodynamical corrections to g_S as well as the following effects which alter the Zeeman energy (see Abragam and Van Vleck[12]): (a) departure from Russell-Saunders coupling; (b) the normal and specific mass-effect corrections to g_L; (c) relativity corrections; and (d) diamagnetic interactions within the atom due to the applied magnetic field. Only effects due to (b) and (c) need be taken into account for the accuracy of the present experiments.

A general expression for g_L which takes the finite mass of the nucleus into account is

$$g_L = (1 - m/M) - (m/ML_z)\langle \Phi | B_z | \Phi \rangle \quad , \tag{9}$$

where $\vec{B} = (1/h) \sum_{i<j} [\vec{r}_i \times \vec{p}_j + \vec{r}_j \times \vec{p}_i]$,

and M is the mass of the nucleus. For the case of a valence p-electron and s-electron core,

$$\frac{\langle B_z \rangle}{L_z} = \tfrac{2}{3} \sum_n \int_0^\infty f_n(r) g(r) r^3 dr \times \int_0^\infty g(r) \frac{df_n}{dr} r^2 dr \quad , \tag{10}$$

where $f_n(r)$ and $g(r)$ are the radial parts of the ns and p wave functions, respectively, and the summation is over occupied orbital s states, each orbital being counted only once. In the case of $1s^2 3p$, the summation has only one term. $\langle B_z \rangle / L_z$ was calculated using hydrogenic wave functions ($Z = 1$) for the $3p$ orbital and a screened hydrogenic function for the $1s$ orbital. The resulting value of $\langle B_z \rangle / L_z$ was $+0.009$. Thus, the value for g_L including both normal and specific mass corrections is

$$g_L = 1 - 0.991 m/M \quad . \tag{11}$$

Margenau[13] has shown that the relativistic correction to the magnetic moment of the electron, expressed in Bohr magnetons, is

$$\Delta\mu = J \Delta g_J = -\frac{(2J+1)^2}{2(J+1)} \frac{\overline{T}}{2mc^2}, \quad \text{for } L = J \pm \tfrac{1}{2}. \tag{12}$$

In addition, Lamb[14] makes the approximation that the average kinetic energy $\overline{T}$ is given by

$$\overline{T} = |2W - W_0| \quad ,$$

where W is the total energy of the state in question, and W_0 is the energy of the corresponding state in hydrogen. This approximation is expected to be an excellent one in the 3^2P state of lithium. From this approximation, $\overline{T}/2mc^2$ was calculated to be 1.57×10^{-6}. The relativistic corrections to the g factors are thus

$$\begin{aligned} \Delta g_J &= -4.18 \times 10^{-6}, \quad \text{for } j = \tfrac{1}{2} \\ \Delta g_J &= -3.35 \times 10^{-6}, \quad \text{for } j = \tfrac{3}{2}. \end{aligned} \tag{13}$$

The corrections applied to Eq. (4) are obtained from the relationships

$$gL = \tfrac{1}{2}(g_{3/2} + g_{1/2}) \quad ,$$

and $g_S = 2g_{3/2} - g_{1/2}$.

The fine-structure interval is expressed as

$$\Delta W = 4384.859(27) \mu_0/\mu_p \text{ kHz}.$$

If the ratio of the Bohr magneton to the magnetic moment of the proton[15] is taken as 657.4481 and a correction of 29.7 ± 1.0 ppm is added to account for the shift in mineral oil, the following result is obtained for the fine-structure interval

$$\Delta W(\mathrm{Li}^7 - 3^2P) = 2882.903(18) \text{ MHz}. \tag{14}$$

The measurement of the $\mathrm{Li}^7 - 4^2P$ fine-structure interval has been made by the same method as used for the 3^2P state of Li^7, and the following results were obtained:

$$\begin{aligned} H_C(\mathrm{Li}^7 - 4^2P) &= 1621.71(15) \text{ kHz}, \\ \Delta W(\mathrm{Li}^7 - 4^2P) &= 1199.65(11) \text{ MHz}. \end{aligned} \tag{15}$$

The loss in resolution caused by overlapping of the four hyperfine components does not permit determination of the interval to the same accuracy as in the 3^2P state.

The accuracy of measuring the fine structure in Li^6 is also limited by the relatively close spacing of the hyperfine levels, and we obtain

$$\begin{aligned} H_C(\mathrm{Li}^6 - 3^2P) &= 3896.89(20) \text{ kHz}, \\ \text{and} \quad \Delta W(\mathrm{Li}^6 - 3^2P) &= 2882.70(15) \text{ MHz}. \end{aligned} \tag{16}$$

Table II lists the fine-structure separations for the 2^2P, 3^2P, and 4^2P states of lithium as well as the corresponding separations in hydrogen. The fine-structure splitting in the $2P$ state of lithium is 91.6% of that in the $2P$ state of hydrogen. The relevant percentages for the $3P$ and $4P$ states are 89.0 and 87.6%, respectively. At first glance, the fact that the lithium fine-structure separations are smaller than those in hydrogen may seem surprising. One might expect that the core penetration in lithium would result in an effective

TABLE II. Fine-structure splittings in Li and H.

Atomic state	Fine-structure splitting (ΔW in cm^{-1})		$\frac{\Delta W_{Li}}{\Delta W_H}$
	Li	H	
$2P$	0.335	0.366	0.916
$3P$	0.0962	0.108	0.890
$4P$	0.0400	0.0456	0.876

nuclear charge greater than unity, and thus a proportionately greater fine structure.

The explanation for this apparently anomalous behavior lies in the magnetic interaction of the p electron with the core electrons. The spin-orbit interaction may be written[2]

$$H_{SO}=\alpha^2\left(Z\sum_i\frac{(\vec{r}_i\times\vec{p}_i)\cdot s_i}{r_i^3}-\sum_i\sum_j\frac{(\vec{r}_{ij}\times\vec{p}_i)\cdot\vec{s}_i}{r_{ij}^3}\right.$$

$$\left.+2\sum_i\sum_j\frac{(\vec{r}_{ij}\times\vec{p}_j)\cdot\vec{s}_i}{r_{ij}^3}\right), \qquad (17)$$

where $\vec{r}_i$, $\vec{p}_i$, and $\vec{s}_i$ are the position, momentum, and spin operators of the ith electron expressed in atomic units, α is the fine-structure constant, z is the nuclear charge, $r_{ij}=|\vec{r}_i-\vec{r}_j|$, and the energies are expressed in rydbergs. The first term in Eq. (17) is the usual spin-orbit interaction of the ith electron in the Coulomb field of the nucleus. The second term is the spin-orbit interaction of the ith electron in the Coulomb field of the other electrons and provides the screening of the nuclear charge. The third term is the interaction of the magnetic moment of the ith electron with the orbital magnetic fields of the other electrons, i.e., the spin-other-orbit coupling. This operator has been evaluated for the $1s^22p$, $1s^23p$, and $1s^24p$ configurations of lithium by Bell and Steward using open-shell variational wave functions. Bell has also obtained results for the first two configurations from Hartree-Fock wave functions, and finds much closer agreement with experimental results. In all cases, the effects of the third term are large enough to account for the reduction of the fine-structure interval from the value for the corresponding interval in hydrogen. However, even though there is qualitative agreement between the theory and experiment, the calculated values differ from measurements by roughly 50%, and there is an obvious need to develop more accurate theoretical methods. It is hoped that the present results will prove useful to test more sophisticated theoretical techniques for the evaluation of two-electron operators.

ACKNOWLEDGMENT

We would like to thank Dr. K. N. Scott of the Department of Chemistry, University of Florida, for providing us with the NMR spectrum which has been used to evaluate the proton resonance frequency in our oil sample, relative to the resonance frequency in water.

APPENDIX: HYPERFINE INTERACTIONS AND CALCULATION OF H_c

The Hamiltonian for the energy of any hyperfine level of a multiplet with respect to the center of gravity of that multiplet can be split into two parts as described in Sec. II, $\mathcal{H}=\mathcal{H}(1)+\mathcal{H}(2)$. The term $\mathcal{H}(1)$ contains the fine-structure interaction and the major part of the Zeeman effect; $\mathcal{H}(2)$ includes all hyperfine interactions and certain small terms that nust be included in the Zeeman effect.

$$\mathcal{H}(1)=g_L\mu_0\vec{L}\cdot\vec{H}+g_S\mu_0\vec{S}\cdot\vec{H}+F,$$

where g_L and g_S are the g factors for the orbital- and spin-magnetic moments of the electrons, respectively, and F is the fine-structure operator.

Diagonalization of $\mathcal{H}(1)$ yields the energies of the $P_{3/2}{}^{-3/2}$ and $P_{1/2}{}^{1/2}$ states. If these energies are equated corresponding to the condition for a level crossing to occur in the absence of hyperfine interactions, it is found that

$$\mu_0H_c=[(g_S+2g_L)/3g_L(g_S+g_L)]\Delta W,$$

where ΔW is the fine-structure interval and H_c is the strength of the field at the point of crossing.

When H_c is large enough to almost completely decouple the nuclear spin I from the electronic angular momentum J, which is the case in the present experiments, $(2I+1)$ level crossings are observed. Each crossing occurs at some field H_i, which is slightly different from H_c. The relationship between H_i, H_c, and the hyperfine energy can be computed from first- and second-order perturbation calculations of $\mathcal{H}(2)$ which employ the eigenfunctions of $\mathcal{H}(1)$ as a basis.

If g_L and g_S are taken to equal 1.0 and 2.0, respectively, the eigenfunctions of $\mathcal{H}(1)$ are related to those at zero magnetic field in a $|JM_J\rangle$ basis by:

$$|\tfrac{3}{2},\ \tfrac{3}{2}\rangle\rightarrow|\tfrac{3}{2},\ \tfrac{3}{2}\rangle,$$

$$|\tfrac{3}{2},\ \tfrac{1}{2}\rangle\rightarrow\alpha|\tfrac{3}{2},\ \tfrac{1}{2}\rangle-\beta|\tfrac{1}{2},\ \tfrac{1}{2}\rangle,$$

$$|\tfrac{3}{2},\ -\tfrac{1}{2}\rangle\rightarrow\gamma|\tfrac{3}{2},\ -\tfrac{1}{2}\rangle-\delta|\tfrac{1}{2},\ -\tfrac{1}{2}\rangle,$$

$$|\tfrac{3}{2},\ -\tfrac{3}{2}\rangle \rightarrow |\tfrac{3}{2},\ -\tfrac{3}{2}\rangle,$$
$$|\tfrac{1}{2},\ \tfrac{1}{2}\rangle \rightarrow \alpha|\tfrac{1}{2},\ \tfrac{1}{2}\rangle + \beta|\tfrac{3}{2},\ \tfrac{1}{2}\rangle, \tag{A1}$$
$$|\tfrac{1}{2},\ -\tfrac{1}{2}\rangle \rightarrow \gamma|\tfrac{1}{2},\ -\tfrac{1}{2}\rangle + \delta|\tfrac{3}{2},\ -\tfrac{1}{2}\rangle,$$

in which the coefficients are

$$\alpha = 0.9701\ ,$$
$$\beta = -0.1715\ , \tag{A2}$$
$$\gamma = 0.9740\ ,$$
$$\delta = -0.2266\ .$$

An explicit expression for $\mathcal{H}(2)$ as a single-electron operator may be written using tensor notation as[16]

$$\mathcal{H}(2) = -2g_N\mu_N\mu_0\vec{I}^{(1)}\cdot\{\vec{L}^{(1)}/r_L{}^3 - \sqrt{10}[\vec{S}^{(1)}\times\vec{C}^{(2)}]^{(1)}/r_S{}^3 - \tfrac{4}{3}\pi\delta(\vec{r})\vec{S}^{(1)}\} + \mu_0\vec{\Delta}\vec{H}^{(1)}\cdot[g_L\vec{L}^{(1)} + g_S\vec{S}^{(1)}] - g_N\mu_N\vec{H}^{(1)}\cdot\vec{I}^{(1)} + \vec{Q}^{(2)}\cdot\vec{U}^{(2)}\ . \tag{A3}$$

The first set of curly brackets includes three terms; the first two relate to energy of interaction of the nuclear moment with the orbital- and spin-magnetic moments of a non-s electron. The Fermi contact energy is represented by the third term which produces a nonzero result only for s electrons. The final term of (A3) is the electric-quadrupole interaction.

The factors $\langle r_L{}^{-3}\rangle$ and $\langle r_S{}^{-3}\rangle$ which appear in (A3) are identical for a single-electron configuration and represent the distance of the electron from the nucleus. For a multielectron system in which configuration interactions are important, $\mathcal{H}(2)$ is allowed to operate upon a sum of all single-electron product wave functions that can be coupled to the nominal configurations by electron-electron Coulomb interactions or by spin-orbit interactions. It can be shown, however, that this procedure is equivalent to using a Hamiltonian of the form of $\mathcal{H}(2)$ operating upon the functions of (A1), provided that $\langle r_L{}^{-3}\rangle$ and $\langle r_S{}^{-3}\rangle$ are not restricted to be the same, and provided that the contact term is replaced by an equivalent operator $3a_c\vec{S}^{(1)}\cdot\vec{I}^{(1)}$ that accounts for the core polarization.[3,17]

The matrix elements for $\mathcal{H}(2)$ $(SLJ'M_{J'}IM_{I'}|\mathcal{H}(2)|SLJM_JIM_I)$, can be written as the sum of the following terms if we define

$$A = (-1)^{I-M_I+J'-M_{J'}}\cdot[(2I+1)I(I+1)(2J'+1)(2J+1)(2L+1)L(L+1)]^{1/2}\times\begin{pmatrix} I & 1 & I \\ -M_{I'} & -q & M_I\end{pmatrix}\begin{pmatrix} J' & 1 & J \\ -M_{J'} & q & M_J\end{pmatrix}. \tag{A4}$$

Dipole-dipole:

$$2Ag_N\mu_N\mu_0\left[(-1)^{J'+S+L}\langle r_L{}^{-3}\rangle\begin{Bmatrix} S & L & J' \\ 1 & J & L\end{Bmatrix} - \langle r_S{}^{-3}\rangle\left[\frac{30(2S+1)S(S+1)}{(2L+3)(2L-1)}\right]^{1/2}\begin{Bmatrix} S & S & 1 \\ L & L & 2 \\ J' & J & 1\end{Bmatrix}\right]. \tag{A5}$$

Core polarization:

$$3Aa_c(-1)^{S+L+J+1}\left[\frac{(2S+1)(S+1)S}{(2L+1)L(L+1)}\right]^{1/2}\begin{Bmatrix} L & S & J' \\ 1 & J & S\end{Bmatrix}. \tag{A6}$$

Zeeman effect:

$$-\mu_0\Delta H(-1)^{J'-m_{J'}+L}[(2J+1)(2J'+1)]^{1/2}\times\begin{pmatrix} J' & 1 & J \\ -M_J & 0 & M_J\end{pmatrix}\left[(-1)^{J'+S}[(2L+1)(L+1)L]^{1/2}\times g_L\begin{Bmatrix} L & J' & S \\ J & L & 1\end{Bmatrix} + (-1)^{J+S}[(2S+1)(S+1)S]^{1/2}\times g_S\begin{Bmatrix} S & J' & L \\ J & S & 1\end{Bmatrix}\right]. \tag{A7}$$

Electric quadrupole:

$$(-1)^{2J'-M_{J'}-I-M_I+S+L+1}\tfrac{1}{2}e^2Q\langle r_Q{}^{-3}\rangle\times\left[\frac{(2I+3)(I+1)(2I+1)(2J+1)(2J'+1)(2L+1)L(L+1)}{I(2I-1)(2L+3)(2L-1)}\right]^{1/2}\times\begin{pmatrix} I & 2 & I \\ -M_{I'} & -q' & M_I\end{pmatrix}\begin{pmatrix} J' & 2 & J \\ -M_{J'} & q & M_J\end{pmatrix}\begin{Bmatrix} S & L & J' \\ 2 & J & L\end{Bmatrix}. \tag{A8}$$

In this expression the average value of $r_Q{}^{-3}$ for the quadrupole term has been assumed different from that of the dipole terms, again to allow for

the effects of configuration interaction. Equation (A5) can be evaluated for a term that is diagonal in J and M_J, then compared to the dipole interaction written in the form $a_J \vec{I} \cdot \vec{J}$ in order to obtain the relationships

$$a_{d3/2} = -2g_N\mu_N\mu_0\left(\tfrac{2}{3}\langle r_L^{-3}\rangle - \tfrac{2}{15}\langle r_S^{-3}\rangle\right),$$

$$a_{d1/2} = -2g_N\mu_N\mu_0\left(\tfrac{4}{3}\langle r_L^{-3}\rangle + \tfrac{4}{3}\langle r_S^{-3}\rangle\right).$$

Also, the usual quadrupole coupling constant b is related to Q by

$$b = [4e^2QJ(2J-1)/15L(L+1)]\langle r_Q^{-3}\rangle .$$

The calculated relationships for the crossings are shown in Table I.

It should be noted that only in cases where $\langle r_L^{-3}\rangle$ is equal to $\langle r_S^{-3}\rangle$ does $a_{d1/2} = 5a_{d3/2}$. At the present time there is insufficient experimental data on the hyperfine constants of lithium to know the accuracy of this relationship. The 5:1 ratio has been used for the second-order terms shown in Table I.

---

†Work supported in part by the National Aeronautics and Space Administration under Grant NGR-33-008-009 and in part by the Joint Services Electronics Program under Contract DA-28-043 AMC-00099(E).

*Present address: University of Florida, Department of Physics and Astronomy, Gainesville, Fla. 32601.

‡Submitted in partial fulfillment for the degree of Doctor of Philosophy at Columbia University, 1967. Present address: United Aircraft Research Laboratories, E. Hartford, Conn. 06108.

§Alfred P. Sloan Research Fellow.

[1]K. L. Bell, Proc. Phys. Soc. (London) 85, 1314 (1965).

[2]K. L. Bell and A. L. Stewart, Proc. Phys. Soc. (London) 83, 1039 (1964).

[3]K. C. Brog, H. Wieder, and T. Eck, Phys. Rev. 153, 91 (1967).

[4]B. Budick, H. Bucka, R. J. Goshen, A. Landman, and R. Novick, Phys. Rev. 147, 1 (1966).

[5]G. Breit, Rev. Mod. Phys. 5, 91 (1933).

[6]T. G. Eck, L. L. Foldy, and H. Wieder, Phys. Rev. Letters 10, 239 (1963).

[7]J. S. M. Harvey, Proc. Roy. Soc. (London) A285, 581 (1965).

[8]G. J. Ritter, Can. J. Phys. 43, 770 (1965).

[9]R. C. Isler, S. Marcus, and R. Novick, following paper, Phys. Rev. 187, 76 (1969).

[10]B. Budick, R. Novick, and A. Lurio, Appl. Opt. 4, 229 (1965).

[11]R. C. Isler, J. Opt. Sci. (to be published).

[12]A. Abragam and J. H. Van Vleck, Phys. Rev. 92, 1448 (1953).

[13]H. Margenau, Phys. Rev. 57, 383 (1940).

[14]W. Lamb, Phys. Rev. 60, 817 (1961).

[15]The resonant frequency of the protons in the oil sample was measured to be 3.7 ppm larger than the resonance frequency of protons in water. Values of the constants used in our analysis are taken from E. R. Cohen and J. W. Du Mond, Rev. Mod. Phys. 37, 537 (1965).

[16]Bruce W. Shore and Donald H. Menzel, Principles of Atomic Spectra (John Wiley & Sons, Inc., New York, 1968).

[17]B. Judd, Proceedings of the Conference on La Structure Hyperfine Magnétique des Atomes et des Molécules, Paris, 1966 (unpublished).